Food Coherence: Measuring Nutritional Quality Through Biophotonic and Metabolic Coherence Signatures

Iulia Koplik* Joel Thorarinson† Allison Hensgen‡

June 2026

Abstract

A carrot from organic soil and a carrot-flavored ultra-processed snack both contain beta-carotene. One emits coherent delayed luminescence for seconds after photoexcitation; the other does not. One supports gut microbial diversity; the other suppresses it. One produces a smooth, low-variance glucose response; the other triggers a spike-and-crash. These are not different properties — they are the same property measured at different scales: the food's organizational coherence, progressively destroyed by industrial processing.

We propose the *Food Coherence Index* (FCI), a multi-scale measurement framework that quantifies nutritional quality through four complementary coherence signatures: (1) *biophotonic coherence*, measured via delayed luminescence decay kinetics after broadband excitation; (2) *molecular coherence*, quantified through antioxidant network completeness and lipid oxidation state; (3) *microbial coherence*, assessed by Shannon diversity, Pielou's evenness, and resilience of the consumer's gut microbiome after ingestion; and (4) *metabolic coherence*, measured through continuous glucose monitoring (CGM) response variability. Each layer captures a distinct scale of food organization, from quantum-level photon emission to organism-level metabolic response. We formalize these four layers using coherence operators from the Coherence Engine framework [Thorarinson et al., 2026a], demonstrate that ultra-processing systematically degrades coherence at every layer, and show that traditional preservation methods — fermentation, lacto-fermentation, dehydration — transform rather than destroy food coherence. We propose an experimental protocol pairing biophoton measurement with 16S microbiome sequencing and CGM monitoring to validate the framework, and outline the operational definition of a Food Coherence Label applicable to consumer products.

Keywords: food coherence; delayed luminescence; biophotons; ultra-processed food; gut microbiome; continuous glucose monitoring; NOVA classification; fermentation; coherence engine; food quality

1 Introduction

The dominant framework for evaluating food quality treats food as a collection of molecular components — macronutrients, micronutrients, vitamins, minerals, additives — each assessable in isolation. A food is "nutritious" if it contains the right molecules in the right quantities. This reductionist model underlies nutritional labeling, dietary guidelines, and the food industry's strategy of fortification: if a processed food lacks vitamin C, add ascorbic acid; if it lacks fiber, add inulin. The implicit assumption is that nutritional value is compositionally determined — that the arrangement, integration, and organizational state of a food's molecular constituents are nutritionally irrelevant.

This assumption is false.

*Coherence Research Group. ORCID: 0009-0005-3765-4811. Corresponding author: iulia.koplik@gmail.com
†Coherence Research Group. ORCID: 0000-0002-0553-842X. joel.thorarinson@conformalmaps.com
‡Coherence Research Group. ORCID: 0009-0008-7247-0307

The most direct evidence comes from Hall et al. [2019], who conducted the first randomized controlled trial comparing ultra-processed and unprocessed diets matched for calories, macronutrients, sugar, sodium, and fiber. Despite compositional equivalence, participants on the ultra-processed diet consumed 508±106 kcal/day more and gained 0.9±0.3 kg over two weeks, while the unprocessed diet group lost 0.9±0.3 kg. The molecular inventory was the same. The organizational state of the food was not.

Epidemiological evidence confirms this at population scale. The EPIC cohort study [Huybrechts et al., 2022] validated the NOVA ultra-processing classification [Monteiro et al., 2019] against biomarkers, finding that ultra-processed food consumption correlates with inflammatory markers, metabolic syndrome, and mortality independent of nutrient composition. Cordova et al. [2023] demonstrated dose-dependent associations between ultra-processed food intake and multimorbidity of cancer and cardiometabolic diseases across European populations. The comprehensive umbrella review of Lane et al. [2024] identified consistent adverse associations across 45 health outcomes, concluding that ultra-processing itself — not merely poor nutrient profiles — drives harm. Meanwhile, preservative food additives show independent associations with type 2 diabetes incidence even after adjusting for overall diet quality [Hasenböhler et al., 2025], and food-grade titanium dioxide nanoparticles induce chromosomal aberrations in human intestinal cells at concentrations encountered in processed foods [Nam et al., 2025].

The NOVA classification [Monteiro et al., 2019] captures the intuition that processing matters, but it is categorical (four groups) and process-defined rather than property-defined. It tells us *how much* a food was processed, not *what was lost*. A continuous, property-based measure of food quality — one that quantifies the organizational state that processing destroys — is missing.

1.1 The Coherence Hypothesis

We propose that what ultra-processing destroys is *coherence*: the coordinated organization of a food's molecular, structural, microbial, and photonic properties that emerges from biological growth and is progressively disrupted by industrial intervention. This is not a metaphor. Coherence is measurable at every scale:

- **Biophotonic scale.** Living and minimally processed foods emit delayed luminescence — coherent photon emission persisting for seconds to minutes after photoexcitation — with characteristic decay kinetics that differ between organic and conventional cultivation, between fresh and degraded samples, and between whole foods and extracted pure substances [Stolz et al., 2019, Popp, 1984].

- **Molecular scale.** Whole foods contain antioxidant networks — systems of polyphenols, carotenoids, vitamins, and cofactors that function synergistically. Processing fragments these networks, leaving isolated compounds that lack the cooperative behavior of the intact system [Barański et al., 2014].

- **Microbial scale.** The gut microbiome responds to food as an ecosystem responding to perturbation. Whole foods support diversity and resilience; ultra-processed foods suppress diversity and reduce recovery capacity [Sonnenburg and Bäckhed, 2016]. The microbiome's response to a meal is itself a coherence measurement: a diverse, resilient community absorbs the perturbation and returns to its baseline; a degraded community does not.

- **Metabolic scale.** Continuous glucose monitoring reveals that glycemic responses to identical foods vary dramatically between individuals [Zeevi et al., 2015] and that the *variability* of the response — not just its peak — carries information about metabolic health [Hall et al., 2018]. Smooth, low-variance glucose curves reflect metabolic coherence; spike-and-crash patterns reflect metabolic incoherence.

These four scales are not independent measurements of different properties. They are measurements of the same property — organizational coherence — at different resolutions. A food that has lost its biophotonic coherence has also lost molecular network integrity, will disrupt microbial coherence upon ingestion, and will produce an incoherent metabolic response. This hierarchical coupling is the central prediction of the Food Coherence framework.

1.2 Connection to the Coherence Engine

The Coherence Engine [Thorarinson et al., 2026a] provides a mathematical framework for measuring whether a complex system is maintaining or losing its structural organization, using a composite operator $\Delta = (P \cdot A \cdot R)/(D+N)$ that combines pattern retention (P), alignment across channels (A), recovery after perturbation (R), drift from baseline (D), and noise growth (N). This framework has been validated across seven physical domains — turbofan engines, cardiac rhythms, industrial processes, power grids, EEG signals, financial time series, and synthetic benchmarks. It has been adapted for biological recovery signatures, where the distinction between true recovery and compensation captures clinically meaningful physiological degradation [Thorarinson et al., 2026b].

We apply the same operator formalism to food quality. The food system — from growth to consumption — is a system whose coherence can be measured, tracked, and compared. The operators map directly:

- **Pattern retention** P: Does the food maintain its characteristic biophotonic emission spectrum, antioxidant profile, and structural integrity over time?
- **Alignment** A: Do the four coherence layers (biophotonic, molecular, microbial, metabolic) move together, or has processing decoupled them?
- **Recovery** R: After environmental perturbation (storage, transport, preparation), does the food system recover its organizational state?
- **Drift** D: How rapidly does the food depart from its freshly harvested baseline?
- **Noise** N: Does the food exhibit increasing randomness in its measurable properties?

The composite Δ thus provides a single, continuous Food Coherence Index (FCI) that integrates information from all four measurement layers.

1.3 Paper Organization

Section 2 develops the biophotonic coherence layer, grounded in the delayed luminescence literature. Section 3 addresses molecular coherence and antioxidant network integrity. Section 4 formalizes microbial coherence using ecological metrics adapted for gut microbiome response. Section 5 develops metabolic coherence through CGM response analysis. Section 6 integrates the four layers into the Food Coherence Index using coherence operators. Section 7 demonstrates that ultra-processing systematically degrades coherence at every layer. Section 8 analyzes traditional preservation methods as coherence transformations rather than coherence destruction. Section 9 proposes an experimental validation protocol. Section 10 outlines the Food Coherence Label. Section 11 addresses limitations and open questions.

2 Biophotonic Coherence

All living biological systems emit ultra-weak photon emission (UPE), also called biophotons, at intensities of 10^1–10^3 photons/s/cm^2 [Cifra and Pospíšil, 2014, Popp and Beloussov, 2003]. When a biological sample is excited by an external light source and the excitation is terminated,

the sample continues to emit photons for seconds to minutes — a phenomenon called *delayed luminescence* (DL). The decay kinetics of this emission carry information about the organizational state of the sample.

2.1 Delayed Luminescence as a Coherence Measure

Stolz et al. [2019] provided a systematic review of delayed luminescence measured by Fluorescence Excitation Spectroscopy (FES) across food samples including wheat kernels, carrots, eggs, and seeds. Their key findings establish DL as a food quality discriminator:

1. **Living vs. extracted.** Whole biological samples emit after excitation at multiple wavelengths (blue, green, yellow, red), while extracted pure chemical substances (sucrose, citric acid) emit only after blue excitation. The breadth of the excitation-emission spectrum reflects the organizational complexity of the sample.

2. **Healthy vs. degraded.** A low emission level and slow decay characterize "healthy or well-differentiated situations" — the intact matrix absorbs and redistributes excitation energy efficiently. High emission with rapid decay indicates degraded organization: the sample cannot maintain coherent energy distribution.

3. **Organic vs. conventional.** Cultivation method influences emission characteristics. The type and intensity of fertilization affect wheat kernel DL, with organic samples showing distinct spectral signatures from conventionally grown samples.

4. **Developmental state.** Wheat seedlings emit differently from dried kernels; the emission pattern tracks physiological development and ripening stage.

These findings map directly onto the coherence framework.

Definition 1 (Biophotonic Coherence)**.** *For a food sample excited at wavelengths $\lambda_1, \ldots, \lambda_k$ and measured by time-resolved photon counting, the biophotonic coherence is:*

$$C_{bio}(t) = \frac{\sum_{j=1}^{k} I_j(t) \cdot \tau_j}{\sum_{j=1}^{k} I_j(0)} \cdot S_{spectral} \tag{1}$$

where $I_j(t)$ is the emission intensity at time t following excitation at λ_j, τ_j is the $1/e$ decay time for channel j, and $S_{spectral} = 1 - JSD(p_{sample} \| p_{reference})$ is the spectral similarity between the sample's excitation-emission profile and a reference profile for the food type at peak freshness, with JSD denoting the Jensen-Shannon divergence.

The numerator captures the total coherent energy storage capacity — how much energy the sample can absorb and slowly release through organized decay. The denominator normalizes by initial emission intensity. The spectral similarity term penalizes samples whose emission profile has deviated from the species-typical pattern.

2.2 Physical Basis

The physical mechanism underlying delayed luminescence in biological systems remains debated. Popp [1984] proposed that DL reflects coherent photon storage in the electromagnetic field of biomolecules, with the organism acting as a coherent source. The alternative view holds that DL arises from energy storage in metastable excited states of molecules such as DNA excimers — bases that do not immediately return to the ground state but form meta-stable configurations far from thermodynamic equilibrium [Lovly et al., 2008]. Under this model, the decay kinetics reflect the complexity and coupling of the molecular landscape, with more organized systems exhibiting longer-lived meta-stable states.

For the Food Coherence framework, the mechanism distinction is operationally secondary. Both models predict the same observable: organized biological systems produce longer-lived, spectrally richer delayed luminescence than degraded or extracted systems. Whether this reflects a coherent photon field or a landscape of coupled metastable states, the measurement discriminates organizational state. This agnosticism parallels the approach of the Coherence Engine [Thorarinson et al., 2026a], which measures coherence without requiring a specific physical model of the system producing it.

Recent work by Benfatto et al. [2021] applied Diffusion Entropy Analysis (DEA) to biophoton time series from germinating seeds and demonstrated anomalous scaling during biological state transitions — departure from the ordinary scaling index $\eta = 0.5$. The transition from crucial events (criticality-driven intermittence) to fractional Brownian motion with stationary infinite memory during germination constitutes a measurable coherence transition in the photon emission signal itself. Dlask et al. [2019] showed that short-time fractal analysis via Hurst exponent estimation reveals negative memory (anti-persistence) in biophoton time series from mung bean seeds, indicating complex temporal organization rather than random decay. These findings support the use of DL as a coherence measure: the temporal structure of the emission encodes the organizational state of the emitter.

2.3 Measurement Protocol for Food DL

Following Stolz et al. [2019], we specify a standardized measurement protocol:

1. Sample preparation: whole food samples, minimally handled, maintained at controlled temperature (20 ± 1°C) and humidity.
2. Sequential excitation at four wavelengths: blue (450 nm), green (530 nm), yellow (590 nm), red (640 nm), each for 10 s.
3. Detection begins 0.2 s after excitation ends (pneumatic shutter control), continuing for 60 s.
4. Record the full decay curve; extract parameters Mw1 (first measurement, initial emission intensity) and R40 (mean of last 40 measurements, residual emission).
5. Repeat across $n \geq 5$ sub-samples; compute mean and coefficient of variation for each parameter.

The ratio R40/Mw1 is a direct coherence indicator: high R40/Mw1 reflects slow, sustained decay (coherent energy redistribution); low R40/Mw1 reflects rapid decay (organizational breakdown). Multiplied by spectral breadth (number of excitation wavelengths producing detectable emission), this yields the biophotonic coherence score C_{bio}.

3 Molecular Coherence

A whole food is not a bag of molecules. It is a structured system in which molecules exist in specific spatial arrangements, concentration gradients, and functional networks. Processing disrupts these arrangements at multiple levels: cell walls are ruptured, enzymes are denatured, lipids are oxidized, and synergistic networks of antioxidants are fragmented.

3.1 Antioxidant Network Coherence

The meta-analysis of Barański et al. [2014] demonstrated that organically grown crops contain 18–69% higher concentrations of antioxidant compounds (polyphenols, phenolic acids, flavanones,

stilbenes, flavones, flavonols, anthocyanins) compared to conventional crops, along with lower cadmium concentrations and lower pesticide residue frequency. These compositional differences reflect cultivation conditions that support or suppress the plant's endogenous antioxidant network.

We define molecular coherence through the integrity of this network:

Definition 2 (Molecular Coherence)**.** *For a food sample with measured concentrations* $\{c_1, \ldots, c_m\}$ *of* m *antioxidant compounds, the molecular coherence is:*

$$C_{mol} = \underbrace{\left(1 - \frac{d_{profile}}{d_{max}}\right)}_{\text{profile similarity}} \cdot \underbrace{\left(1 - \frac{TBARS}{TBARS_{max}}\right)}_{\text{oxidative integrity}} \cdot \underbrace{H_{norm}(\mathbf{c})}_{\text{network diversity}} \tag{2}$$

where $d_{profile}$ *is the Euclidean distance between the sample's antioxidant profile vector* $\mathbf{c}$ *and the reference profile for the food type at harvest, TBARS is thiobarbituric acid reactive substances (a lipid oxidation marker), and* H_{norm} *is the normalized Shannon entropy of the antioxidant concentration vector.*

The three multiplicative terms capture complementary aspects of molecular organization:

- Profile similarity: has the relative balance of antioxidants been preserved?
- Oxidative integrity: have lipids and other oxidation-sensitive molecules been degraded?
- Network diversity: does the sample maintain a broad spectrum of protective compounds, or has processing reduced it to a few dominant molecules?

A fortified ultra-processed food may score high on total antioxidant capacity (because ascorbic acid was added) while scoring low on molecular coherence (because the native network was destroyed and replaced by a single compound). This distinction — between total content and organizational integrity — is precisely what the coherence framework captures and conventional nutritional analysis misses.

4 Microbial Coherence

The human gut microbiome is an ecosystem of $\sim 10^{13}$ microorganisms whose composition, diversity, and functional capacity respond to dietary input within hours [Sonnenburg and Bäckhed, 2016]. The microbiome's response to a meal is itself a measurement of the meal's organizational quality: a diverse, resilient ecosystem absorbs the perturbation of a meal and returns to its baseline configuration; a degraded ecosystem exhibits large, persistent shifts.

4.1 The Gut Microbiome as a Coherence Detector

Fülling et al. [2019] reviewed the mechanisms by which gut microbes signal to the brain through the vagus nerve, enteroendocrine cells, and microbial metabolites (short-chain fatty acids, neurotransmitters, tryptophan metabolites). Mirzaei et al. [2021] documented the role of microbiota-derived short-chain fatty acids — butyrate, propionate, acetate — in nervous system function, demonstrating that gut microbial metabolism has systemic physiological consequences mediated by specific molecular signals. Lombardo-Hernandez et al. [2025] introduced the concept of the "bioelectrical microbiome," demonstrating that bacteria communicate through membrane potential dynamics, ion channels, and electrical signaling that directly modulates neural excitability via vagal afferents. These findings establish the gut microbiome not merely as a passive recipient of food but as an active signal-processing system whose bioelectrical and metabolic outputs reflect the quality of its inputs.

The ecological coherence of this system can be formalized:

Definition 3 (Microbial Coherence)**.** *For a subject's gut microbiome measured at time t by 16S rRNA gene sequencing with operational taxonomic unit (OTU) abundances $\{n_1, \ldots, n_s\}$, the microbial coherence is:*

$$C_{micro}(t) = H'(t) \cdot J(t) \cdot R(t, t_0) \tag{3}$$

where:

$$H'(t) = -\sum_{i=1}^{s} p_i(t) \log p_i(t) \quad \textit{(Shannon diversity index)} \tag{4}$$

$$J(t) = \frac{H'(t)}{\log s(t)} \quad \textit{(Pielou's evenness)} \tag{5}$$

$$R(t, t_0) = 1 - d_{BC}(\mathbf{p}(t), \mathbf{p}(t_0)) \quad \textit{(resilience)} \tag{6}$$

with $p_i(t) = n_i(t)/\sum_j n_j(t)$ the relative abundance of OTU i, $s(t)$ the observed species richness, and d_{BC} the Bray-Curtis dissimilarity between the current and baseline community compositions [Shannon, 1948, Pielou, 1966].

Shannon diversity H' measures the information content of the community composition — how many effective species are present and how evenly they are distributed. Pielou's evenness J normalizes this by the theoretical maximum, penalizing communities dominated by a few taxa. The resilience term R measures how quickly and completely the community returns to its pre-meal baseline after the perturbation of eating.

A high-coherence meal is one that the microbiome absorbs without large or persistent changes in community structure. An ultra-processed meal, by contrast, drives rapid shifts in composition — suppressing butyrate-producing *Firmicutes*, promoting pro-inflammatory *Proteobacteria*, and reducing overall diversity — with slow or incomplete recovery [Sonnenburg and Bäckhed, 2016]. The concept of tipping elements in the human intestinal ecosystem [Lahti et al., 2014] suggests that repeated low-coherence meals can push the microbiome past bistable thresholds into alternative stable states from which recovery requires active intervention.

This connects directly to the ecological resilience framework of Holling [1973] and the microbial resistance-resilience analysis of Shade et al. [2012]: a coherent ecosystem absorbs perturbation and recovers; an incoherent one amplifies perturbation and drifts to new states.

4.2 Microbiome Response as Meal Quality Signal

The practical implication is that the microbiome itself can serve as a food quality sensor. Given a standardized pre-meal baseline, the magnitude and duration of post-meal community perturbation quantifies the meal's coherence impact. We define:

$$\text{Meal Impact}(m) = \int_{t_{\text{meal}}}^{t_{\text{meal}}+T} d_{\text{BC}}(\mathbf{p}(\tau), \mathbf{p}(t_{\text{pre}}))\, d\tau \tag{7}$$

where T is a standardized observation window (24–48 hours). Low meal impact indicates a coherent food that integrates smoothly with the existing microbial community; high meal impact indicates a disruptive food.

5 Metabolic Coherence

Continuous glucose monitoring (CGM) provides a high-resolution window into the body's metabolic response to food. The temporal profile of glucose after a meal — its peak amplitude, time to peak, rate of decline, nadir depth, and return to baseline — encodes information about the metabolic coherence of both the food and the consumer.

5.1 Glycemic Variability as Incoherence

Hall et al. [2018] identified distinct "glucotypes" by clustering CGM patterns, finding that even normoglycemic individuals fall into low, moderate, and severe variability groups. Zeevi et al. [2015] demonstrated that identical foods produce dramatically different glycemic responses across individuals, driven by gut microbiome composition, meal timing, physical activity, and sleep. These findings establish that the glucose response to a meal is a joint function of the food's properties and the consumer's metabolic state.

We define metabolic coherence through the regularity and recoverability of the glucose response:

Definition 4 (Metabolic Coherence)**.** *For a CGM glucose trace $g(t)$ during the postprandial window $[t_{meal}, t_{meal} + 4h]$, the metabolic coherence is:*

$$C_{met} = \frac{1}{1 + CV_g} \cdot \frac{1}{1 + MAGE/\bar{g}} \cdot \exp\left(-\frac{\tau_{rec}}{\tau_{ref}}\right) \tag{8}$$

where CV_g is the coefficient of variation of glucose over the window, MAGE is the Mean Amplitude of Glycemic Excursions [Service et al., 1970], $\bar{g}$ is the mean glucose, τ_{rec} is the time for glucose to return within one standard deviation of the pre-meal baseline, and τ_{ref} is a reference recovery time (90 minutes for healthy adults [Danne et al., 2017]).

The three multiplicative terms capture:

- **Variability suppression:** Low CV_g indicates a smooth, well-regulated response. High CV_g indicates oscillatory or chaotic glucose dynamics.
- **Excursion control:** Low MAGE relative to mean glucose indicates that the metabolic system absorbed the food without large perturbations. High relative MAGE indicates poor glycemic buffering.
- **Recovery speed:** Rapid return to baseline reflects intact metabolic coherence. Prolonged elevation or reactive hypoglycemia reflects degraded regulation.

This connects to the recovery half-life concept developed in Thorarinson et al. [2026b]: the time for a system to return halfway to its baseline state is a direct measure of its coherence, and increasing recovery time is an early warning signal of functional degradation [Scheffer et al., 2009].

5.2 Food–Microbiome–Metabolism Coupling

Zeevi et al. [2015] showed that microbiome composition is a stronger predictor of individual glycemic response than food composition alone. This finding supports the multi-layer coherence hypothesis: a food's metabolic coherence score is not an intrinsic property of the food but an emergent property of the food-microbiome-metabolism system. Ultra-processed foods score low on metabolic coherence partly because they disrupt the microbial layer (Section 4), which in turn degrades metabolic regulation. The four coherence layers are hierarchically coupled, not independent.

6 The Food Coherence Index

We integrate the four coherence layers into a single composite measure using the coherence operator formalism.

6.1 Composite Operator

The Coherence Engine [Thorarinson et al., 2026a] defines the composite coherence as $\Delta = (P \cdot A \cdot R)/(D + N)$. For food coherence, we adapt this operator to the four-layer measurement framework:

Definition 5 (Food Coherence Index)**.** *The Food Coherence Index for a food sample f evaluated at time t after harvest is:*

$$FCI(f,t) = \frac{P_f(t) \cdot A_f(t) \cdot R_f(t)}{D_f(t) + N_f(t)} \tag{9}$$

where the operators are defined in terms of the four coherence layers as:

$$P_f(t) = \frac{C_{bio}(t)}{C_{bio}(0)} \cdot \frac{C_{mol}(t)}{C_{mol}(0)} \tag{10}$$

$$A_f(t) = \rho\left(C_{bio}(t), C_{mol}(t), C_{micro}(t), C_{met}(t)\right) \tag{11}$$

$$R_f(t) = \frac{1}{4} \sum_{l \in \{bio,\ mol,\ micro,\ met\}} \frac{C_l(t+\delta)}{C_l(t)} \tag{12}$$

$$D_f(t) = \frac{1}{T} \int_0^t \left| \frac{d}{ds} \left(\frac{C_{bio}(s) + C_{mol}(s)}{2} \right) \right| ds \tag{13}$$

$$N_f(t) = CV(\{C_l\}_{l \in layers}) \tag{14}$$

In Equation (10), pattern retention is the product of biophotonic and molecular coherence ratios relative to the freshly-harvested reference ($t = 0$). In Equation (11), alignment is the correlation across all four layers — when coherence degrades at one layer but not others, alignment drops, indicating decoupled degradation (e.g., a food that has been chemically stabilized to preserve molecular markers while its biophotonic coherence has collapsed). In Equation (12), recovery measures whether the food system restores coherence after a standardized perturbation (e.g., temperature cycling or mechanical stress). In Equation (13), drift captures the rate of ongoing degradation. In Equation (14), noise measures the inconsistency across layers.

The FCI is a continuous, dimensionless score that decreases monotonically under processing and degradation but — critically — can *increase* under fermentation, where biological transformation creates new organizational coherence (Section 8).

7 Ultra-Processing as Coherence Destruction

The NOVA classification [Monteiro et al., 2019] defines ultra-processed foods (Group 4) as "industrial formulations made entirely or mostly from substances derived from foods and additives, with little if any intact Group 1 food." This definition is process-based. The Food Coherence framework reframes ultra-processing as *systematic coherence destruction across all four measurement layers*, providing a property-based characterization that explains the epidemiological harm.

7.1 Layer-by-Layer Degradation

Biophotonic layer. Stolz et al. [2019] found that extracted pure chemical substances (sucrose, citric acid) emit delayed luminescence only after blue excitation, compared to whole biological samples that emit across the full visible spectrum. Ultra-processing reduces a food to its extracted components — starches, sugars, oils, isolates — each of which has lost the spectral breadth of the intact organism. The prediction is quantitative: C_{bio} decreases monotonically with processing intensity, and the spectral similarity term S_{spectral} drops toward zero as the emission profile diverges from the whole-food reference.

Molecular layer. Industrial processing fragments antioxidant networks through heat denaturation, solvent extraction, hydrogenation, and chemical modification. A whole grain contains hundreds of synergistic phytochemicals in their native spatial arrangement within the bran, germ, and endosperm; refined flour retains only the starch fraction. Fortification with isolated vitamins restores *content* but not *coherence*: the network diversity term H_{norm} collapses to near-zero when a single added compound dominates the antioxidant profile.

Microbial layer. Ultra-processed diets reduce gut microbiome diversity [Sonnenburg and Bäckhed, 2016], suppress butyrate production [Mirzaei et al., 2021], and increase the proportion of pro-inflammatory taxa. The microbial coherence score C_{micro} decreases through all three terms: Shannon diversity drops, evenness drops (a few fast-growing taxa dominate), and post-meal resilience decreases (the community takes longer to recover from the perturbation of an ultra-processed meal). The nonalcoholic fatty liver disease association documented by Zelber-Sagi et al. [2022] may reflect cumulative microbial coherence degradation.

Metabolic layer. Ultra-processed foods produce larger glycemic excursions, higher variability, and slower recovery than whole-food equivalents [Hall et al., 2019]. The metabolic coherence score C_{met} captures this: CV_g increases, MAGE increases, and τ_{rec} lengthens. The Hall 2019 trial is particularly informative because the diets were macronutrient-matched: the metabolic incoherence of the ultra-processed diet cannot be attributed to compositional differences.

7.2 The Degradation Trajectory

Figure 1 illustrates the coherence trajectory from whole food to ultra-processed product. The key insight is that coherence loss is *monotonic but non-uniform across layers*: molecular coherence (heat-stable compounds) may persist after biophotonic coherence (thermolabile organizational states) has collapsed, creating a window in which the food appears nutritionally adequate by compositional analysis while having lost its organizational integrity. This window — where the food looks the same but behaves differently — is precisely the gap that the Hall 2019 trial detected and that the FCI is designed to quantify.

8 Fermentation as Coherence Transformation

Traditional food preservation methods — fermentation, lacto-fermentation, controlled dehydration, pickling, curing — are often grouped with industrial processing under the assumption that all processing degrades food quality. The coherence framework reveals a crucial distinction: *fermentation transforms coherence rather than destroying it.*

8.1 The Transformation Principle

Fermentation introduces microbial communities into the food matrix, initiating controlled biochemical transformations: lactobacilli convert sugars to lactic acid, yeasts produce ethanol and CO_2, *Aspergillus* species break down proteins and starches. These are not random degradations — they are coordinated metabolic processes that create new organizational structures [Marco et al., 2017, Dimidi et al., 2019].

Karimi et al. [2026] demonstrated through metabolic modeling that fermented food microbial communities exhibit complex metabolic interdependencies — cross-feeding networks, syntrophic relationships, and competitive exclusion dynamics — that constitute a form of ecological coherence within the food itself. The ethanol-lactate transition of *Lachancea thermotolerans* during fermentation, for instance, reflects a coordinated metabolic shift, not random chemical degradation.

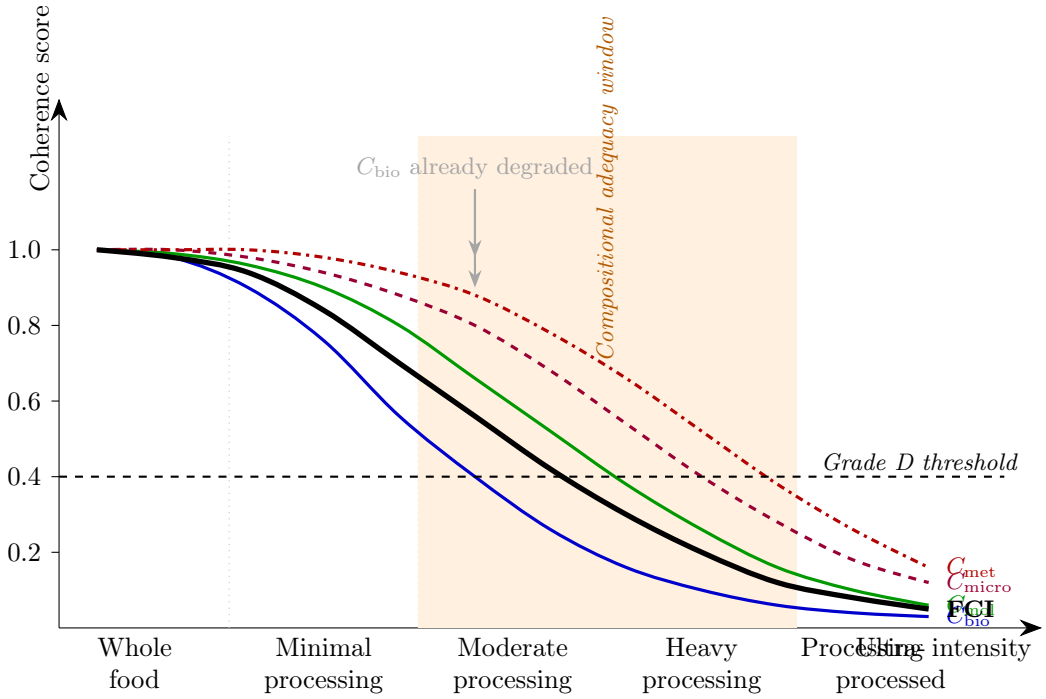

Figure 1: **Coherence degradation trajectory from whole food to ultra-processed product.** Each layer degrades at a different rate under processing, with biophotonic coherence (most sensitive to organizational disruption) declining first and metabolic coherence (measured in the consumer, not the food) declining last. The shaded region represents the "compositional adequacy window" where conventional nutritional analysis detects no deficit but the FCI has already dropped below threshold. UPF: ultra-processed food.

8.2 Layer-by-Layer Analysis of Fermentation

Biophotonic layer. Fermented foods present a distinct delayed luminescence profile from both fresh and degraded foods. The fermentation process creates new metastable molecular configurations — polyphenol-protein complexes in wine, melanoidin networks in fermented soy, exopolysaccharide matrices in kefir — that alter the energy absorption and emission landscape. The prediction is that fermented foods exhibit different C_{bio} profiles from fresh foods of the same origin, but *not* lower overall coherence: the spectral signature changes (lower spectral similarity to the fresh reference) while the decay kinetics remain long-lived (high R40/Mw1).

Molecular layer. Fermentation creates bioactive compounds not present in the starting material — conjugated linoleic acid from dairy fermentation, bioactive peptides from protein hydrolysis, B-vitamins from bacterial synthesis. The molecular coherence score may decrease in profile similarity (the antioxidant profile changes) while increasing in network diversity (new functional compounds are added). The net C_{mol} depends on whether the fermentation creates more organizational complexity than it destroys.

Microbial layer. Fermented foods introduce viable microorganisms and their metabolic products into the gut, directly supporting microbial coherence. Dimidi et al. [2019] reviewed evidence that fermented food consumption is associated with increased gut microbiome diversity and improved gastrointestinal function. The microbial coherence response to a fermented food meal is predicted to show higher evenness and faster recovery than the response to the same food unfermented.

Metabolic layer. Fermentation pre-digests complex carbohydrates, reducing glycemic load and smoothing the glucose response curve. Sourdough fermentation of wheat, for instance, reduces the glycemic index relative to yeast-leavened bread through organic acid production and starch modification. The metabolic coherence score C_{met} is predicted to be higher for fermented than unfermented versions of the same food.

8.3 The Coherence Transformation Operator

We formalize the distinction between destructive processing and transformative processing through a transformation operator:

$$T_{\text{process}}(f) = \frac{\text{FCI}(f_{\text{processed}})}{\text{FCI}(f_{\text{raw}})} \tag{15}$$

When $T < 1$, the process has destroyed coherence (ultra-processing). When $T \approx 1$, the process has preserved coherence (minimal processing, proper storage). When $T > 1$, the process has *created* coherence (successful fermentation, sprouting, controlled aging). This operator provides a principled distinction between processing methods: not all transformation is degradation.

Figure 2 illustrates how fermentation navigates the coherence landscape differently from ultra-processing, with the food system traversing a path through reduced molecular similarity but increased ecological and metabolic coherence.

9 Experimental Protocol

We propose a three-phase experimental protocol to validate the Food Coherence framework.

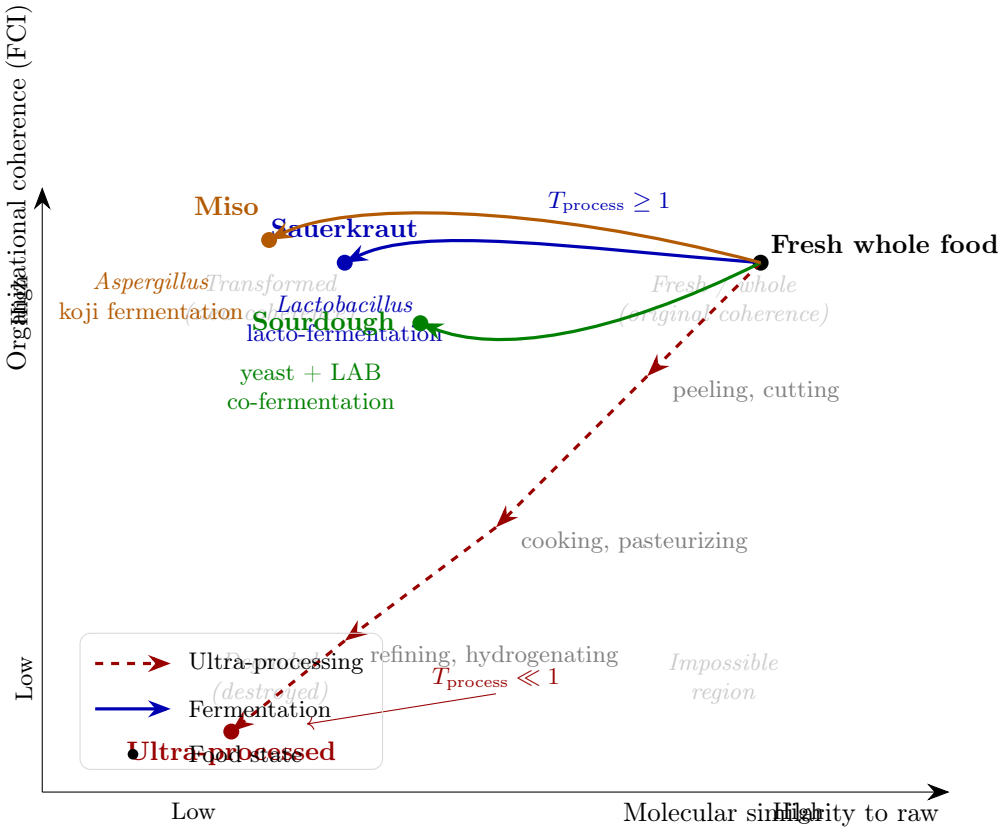

Figure 2: **Fermentation as coherence transformation.** Unlike ultra-processing, which degrades all four coherence layers monotonically (dashed arrows), fermentation (solid arrows) transforms the food's coherence profile: biophotonic and molecular signatures change (the food is different) but overall organizational coherence is maintained or enhanced. The fermented state occupies a different region of the coherence landscape from either the fresh or degraded states. Three traditional fermentation processes are shown: lacto-fermentation of vegetables, sourdough fermentation of grain, and koji (Aspergillus) fermentation of soy.

9.1 Phase 1: Biophotonic Validation

Objective. Establish that delayed luminescence discriminates between food samples of known quality differences.

Design. Select five food categories (wheat, carrot, apple, egg, milk) with samples from: (a) organic cultivation, (b) conventional cultivation, (c) minimally processed (peeled, cut), (d) moderately processed (cooked, pasteurized), and (e) ultra-processed (refined, reconstituted, additive-laden). Measure DL via FES for all samples using the protocol in Section 2. Compute C_{bio} for each sample.

Prediction. C_{bio} will decrease monotonically from (a) to (e), with the largest drop between (c) and (d) (cooking/pasteurization disrupts organizational states) and (d) and (e) (ultra-processing eliminates remaining coherent structures).

Controls. Include inert reference samples (glass, pure sucrose solution) and freshly harvested reference samples for spectral similarity computation.

9.2 Phase 2: Microbiome–Metabolic Coupling

Objective. Demonstrate that biophotonic coherence predicts microbiome and metabolic response.

Design. Crossover trial: $n = 20$ participants consume a whole-food meal and a macronutrient-matched ultra-processed meal (following the Hall 2019 protocol) on separate occasions, separated by a 2-week washout. For each meal:

- Measure food C_{bio} before consumption.
- Measure gut microbiome via 16S sequencing at baseline ($t = 0$), $t = 6$h, $t = 24$h, $t = 48$h.
- Measure glucose via CGM throughout the 48h window.
- Compute $C_{\text{micro}}(t)$ and C_{met} for each meal.

Primary hypothesis. Higher food C_{bio} predicts higher post-meal C_{micro} and C_{met} (cross-layer coupling).

Secondary hypothesis. The alignment operator A_f is higher for whole-food meals than ultra-processed meals (all four layers move together for coherent foods; for incoherent foods, the layers are decoupled).

9.3 Phase 3: Fermentation Comparison

Objective. Demonstrate that fermented foods exhibit $T_{\text{process}} \geq 1$ while ultra-processed versions of the same starting material exhibit $T_{\text{process}} < 1$.

Design. Select three food pairs: (a) raw cabbage vs. sauerkraut vs. coleslaw with preservatives; (b) whole wheat flour vs. sourdough bread vs. white bread with additives; (c) raw soybeans vs. miso vs. soy protein isolate. Measure all four coherence layers for each sample and compute FCI and T_{process}.

Prediction. Fermented products (sauerkraut, sourdough, miso) will show $T_{\text{process}} \geq 1$; ultra-processed products (preserved coleslaw, white bread, soy isolate) will show $T_{\text{process}} \ll 1$.

10 Toward a Food Coherence Label

The practical application of the FCI is a consumer-facing Food Coherence Label that communicates the organizational quality of a food product using a single letter grade derived from the composite score.

10.1 Operational Definition

We propose a five-tier grading system:

Table 1: Proposed Food Coherence Label tiers. Thresholds are preliminary and require empirical calibration through the Phase 1–3 protocol.

Grade	FCI Range	Description
A	≥ 0.8	High coherence. Fresh, whole, or traditionally preserved food with intact organizational structure at all four measurement layers.
B	$[0.6, 0.8)$	Moderate coherence. Minimally processed or well-fermented food. Some layer degradation but overall structural integrity maintained.
C	$[0.4, 0.6)$	Partial coherence. Moderately processed food. Biophotonic layer degraded; molecular and metabolic layers may be partially intact.
D	$[0.2, 0.4)$	Low coherence. Heavily processed food. Multiple layers degraded. May retain molecular content (fortified) without organizational integrity.
F	< 0.2	Minimal coherence. Ultra-processed food with little remaining organizational structure. Compositional adequacy does not imply nutritional coherence.

10.2 Relationship to Existing Systems

The Food Coherence Label is complementary to, not a replacement for, existing nutritional information systems:

- **vs. Nutri-Score:** Nutri-Score evaluates compositional content (calories, sugar, fiber, protein). FCI evaluates organizational state. A food could score A on Nutri-Score and D on FCI (fortified ultra-processed product with good macronutrient profile but destroyed coherence).
- **vs. NOVA:** NOVA classifies by process intensity (four groups). FCI quantifies the property that processing destroys (continuous scale). NOVA tells you what was done to the food; FCI measures what resulted.
- **vs. Organic certification:** Organic certification governs cultivation method. FCI measures the output state. An organically grown crop that is then ultra-processed would receive organic certification but a low FCI.

10.3 Implementation Pathway

The primary barrier to deployment is measurement cost. Biophotonic measurement requires specialized FES instrumentation currently available only in research laboratories. We propose a phased deployment:

1. **Phase I (research):** Establish reference DL profiles for major food categories using laboratory FES. Build the calibration database.
2. **Phase II (proxy development):** Identify molecular and spectroscopic proxies for biophotonic coherence — measurable with cheaper instruments (NIR spectroscopy, fluorescence spectroscopy) — and validate against FES-derived C_{bio}.
3. **Phase III (consumer deployment):** Deploy the proxy-based FCI using existing food testing infrastructure. The consumer label reports the FCI grade; the full four-layer breakdown is available as a detailed report.

11 Limitations and Open Questions

11.1 Measurement Challenges

Biophotonic layer. FES instrumentation is expensive and sensitive to environmental conditions (temperature, ambient light, electromagnetic interference). The reproducibility of DL measurements across laboratories needs systematic characterization. The Stolz 2019 review reports good within-laboratory reproducibility but inter-laboratory comparisons are sparse.

Microbial layer. 16S rRNA sequencing provides taxonomic resolution but not functional information. Shotgun metagenomics would capture functional capacity but at higher cost. The temporal dynamics of post-meal microbiome shifts are under-characterized: the optimal sampling schedule for microbial coherence assessment is unknown.

Metabolic layer. CGM accuracy varies across devices and glucose ranges. Inter-individual variability in glycemic response [Zeevi et al., 2015] means that metabolic coherence scores are not properties of the food alone but of the food-consumer pair. Population-level normalization is needed.

11.2 Theoretical Limitations

Mechanism ambiguity. The biophotonic coherence measure is agnostic to the physical mechanism of delayed luminescence. This is operationally useful but scientifically unsatisfying: without a mechanistic model, the framework cannot predict which specific processing steps will degrade coherence, only detect degradation after the fact.

Confounding. Ultra-processed foods differ from whole foods in multiple ways beyond organizational coherence: additive content, palatability, eating speed, satiety signaling. The Hall 2019 trial controlled for macronutrient composition but not for these other factors. The contribution of organizational coherence *per se* to health outcomes, as distinct from the contribution of specific additives or behavioral factors, remains to be isolated.

Individual variation. Microbial and metabolic coherence scores are inherently individual-specific. The same food will produce different coherence profiles in different consumers, depending on their baseline microbiome composition, metabolic health, and genetic background. Whether food-level FCI (based on biophotonic and molecular layers) reliably predicts consumer-level response requires empirical validation.

11.3 Ethical Considerations

A Food Coherence Label could have significant economic consequences for food manufacturers, retailers, and agricultural producers. Low-FCI products may include affordable staples for low-income populations, and a labeling system that stigmatizes these products without providing accessible high-FCI alternatives could exacerbate food inequality. The framework should be deployed alongside policies that make high-coherence food economically accessible, not as a standalone consumer information tool.

12 Conclusion

The food quality problem has been stated backwards. The question is not "what molecules does this food contain?" but "what organizational state is this food in?" A whole carrot and a reconstituted carrot-flavored product may share the same molecular inventory, but they occupy fundamentally different states of organizational coherence — a difference measurable through delayed luminescence, antioxidant network integrity, microbiome response, and glucose dynamics.

The Food Coherence Index provides the first integrated, continuous measure of this organizational state, bridging the gap between the categorical NOVA classification and the reductionist nutritional label. The experimental program we propose is feasible with existing instrumentation and would generate the calibration data needed for a consumer-facing Food Coherence Label.

Fermentation — humanity's oldest food technology — emerges from this framework not as a form of processing but as a form of organization: a controlled biological transformation that can increase the coherence of the food system rather than destroying it. This distinction between destruction and transformation, invisible to compositional analysis, is precisely what the coherence framework makes measurable.

The central prediction is testable: if the framework is correct, then biophotonic coherence of a food sample, measurable before consumption, will predict the magnitude and quality of the consumer's microbiome and metabolic response — because these are different-scale measurements of the same underlying property. If this prediction holds, the Food Coherence Label becomes not just a quality indicator but a health-relevant signal derived from the physics of organized matter.

Acknowledgments

The authors thank the Forschungsinstitut KWALIS for their foundational work on delayed luminescence measurement in food systems, and the investigators of the Hall 2019 NIH trial for making their protocol publicly available. The Coherence Engine framework underlying this work was developed with support from the coherence research group.

References

Marcin Barański, Dominika Średnicka Tober, Nikolaos Volakakis, Chris Seal, Roy Sanderson, Gavin B Stewart, Charles Benbrook, Bruno Biavati, Emilia Markellou, Charilaos Giotis, et al. Higher antioxidant and lower cadmium concentrations and lower incidence of pesticide residues in organically grown crops: A systematic literature review and meta-analyses. *British Journal of Nutrition*, 112(5):794–811, 2014. doi: 10.1017/S0007114514001366.

Maurizio Benfatto, Elisabetta Pace, Catalina Curceanu, Alessandro Scordo, Stefano Lupi, and Paolo Grigolini. Biophotons and emergence of quantum coherence — a diffusion entropy analysis. *Entropy*, 23(5):554, 2021. doi: 10.3390/e23050554.

Michal Cifra and Pavel Pospíšil. Ultra-weak photon emission from biological samples: Definition, mechanisms, properties, detection and applications. *Journal of Photochemistry and Photobiology B: Biology*, 139:2–10, 2014. doi: 10.1016/j.jphotobiol.2014.02.009.

Reynalda Cordova, Nathalie Kliemann, Inge Huybrechts, Fernanda Rauber, Elias P Vamos, Renata B Levy, and Heinz Freisling. Consumption of ultra-processed foods and risk of multimorbidity of cancer and cardiometabolic diseases: A multinational cohort study. *The Lancet Regional Health – Europe*, 35:100771, 2023. doi: 10.1016/j.lanepe.2023.100771.

Thomas Danne, Revital Nimri, Tadej Battelino, Richard M Bergenstal, Kelly L Close, J Hans DeVries, Satish Garg, Lutz Heinemann, Ira Hirsch, Stephanie A Amiel, et al. International consensus on use of continuous glucose monitoring. *Diabetes Care*, 40(12):1631–1640, 2017. doi: 10.2337/dc17-1600.

Eirini Dimidi, Sharon R Cox, Megan Rossi, and Kevin Whelan. Fermented foods: Definitions and characteristics, impact on the gut microbiota and effects on gastrointestinal health and disease. *Nutrients*, 11(8):1806, 2019. doi: 10.3390/nu11081806.

Martin Dlask, Jaromír Kukal, and Michal Cifra. Short-time fractal analysis of biological autoluminescence. *bioRxiv*, 2019. doi: 10.1101/798074.

Christine Fülling, Timothy G Dinan, and John F Cryan. Gut microbe to brain signaling: What happens in vagus.... *Neuron*, 101(6):998–1002, 2019. doi: 10.1016/j.neuron.2019.02.008.

Heather Hall, Dalia Perelman, Alessandra Breschi, Patricia Limcaoco, Ryan Kellogg, Tracey McLaughlin, and Michael Snyder. Glucotypes reveal new patterns of glucose dysregulation. *PLOS Biology*, 16(7):e2005143, 2018. doi: 10.1371/journal.pbio.2005143.

Kevin D Hall, Alexis Ayuketah, Robert Brychta, Hongyi Cai, Tom Cassimatis, Kong Y Chen, Stephanie T Chung, Elise Costa, Amber Courville, Valerie Darcey, et al. Ultra-processed diets cause excess calorie intake and weight gain: An inpatient randomized controlled trial of ad libitum food intake. *Cell Metabolism*, 30(1):67–77, 2019. doi: 10.1016/j.cmet.2019.05.008.

Anaïs Hasenböhler, Bernard Srour, Nasser Laouali, Léopold K Fezeu, and Mathilde Touvier. Associations between preservative food additives and type 2 diabetes incidence in the NutriNet-Santé prospective cohort. *Nature Communications*, 16:4812, 2025. doi: 10.1038/s41467-025-67360-w.

Crawford S Holling. Resilience and stability of ecological systems. *Annual Review of Ecology and Systematics*, 4:1–23, 1973.

Inge Huybrechts, Fernanda Rauber, Géraldine Nicolas, Corinne Casagrande, Nathalie Kliemann, Carine Biessy, Véronique Chajès, and Heinz Freisling. Characterization of the degree of food processing in the European Prospective Investigation into Cancer and Nutrition: Application of the NOVA classification and validation using selected biomarkers of food processing. *Frontiers in Nutrition*, 9:1035580, 2022. doi: 10.3389/fnut.2022.1035580.

Elham Karimi, Bart van den Bogaard, Arlete Mendes Ferreira, Kiran R Patil, and Richard A Notebaart. Microbiome metabolic modeling as a tool for innovation in fermented foods. *Current Opinion in Food Science*, 62:101264, 2026. doi: 10.1016/j.cofs.2025.101264.

Leo Lahti, Jarkko Salojärvi, Anne Salonen, Marten Scheffer, and Willem M de Vos. Tipping elements in the human intestinal ecosystem. *Nature Communications*, 5:4344, 2014. doi: 10.1038/ncomms5344.

Melissa M Lane, Elizabeth Gamage, Shutong Du, Deborah N Ashtree, Amelia J McGuinness, Sarah Gauci, Phillip Baker, Mark Lawrence, Casey M Rebholz, Bernard Srour, et al. Ultra-processed food exposure and adverse health outcomes: Umbrella review of epidemiological meta-analyses. *BMJ*, 384:e077310, 2024. doi: 10.1136/bmj-2023-077310.

Juan Lombardo-Hernandez, Jesús Mansilla-Guardiola, Stefano Geuna, and Deepak L Bhatt. New insights in the gut–brain axis: The role of bioelectrical microbiome. *Current Opinion in Food Science*, 66:101353, 2025. doi: 10.1016/j.cofs.2025.101353.

M V Lovly, R S Murugan, and N P Kishore. Biophoton emission and the effect of electromagnetic fields on living cells. *Indian Journal of Experimental Biology*, 46(5):371–377, 2008.

Maria L Marco, Dustin Heeney, Sylvie Binda, Christopher J Cifelli, Paul D Cotter, Benoit Foligné, Michael Gänzle, Remco Kort, Gonçalo Pasin, Anne Pihlanto, et al. Health benefits of fermented foods: Microbiota and beyond. *Current Opinion in Biotechnology*, 44:94–102, 2017. doi: 10.1016/j.copbio.2016.11.010.

Rasoul Mirzaei, Behrouz Bouzari, Seyed Mojtaba Hashemi, Ariadna Gonzalez, Mahdi Zarrabi, Foad Badrzadeh, Fatemeh Karimi, Ali Majidi, Masoumeh Valizadeh, Hossein Kianpour, et al. Role of microbiota-derived short-chain fatty acids in nervous system disorders. *Biomedicine & Pharmacotherapy*, 139:111661, 2021. doi: 10.1016/j.biopha.2021.111661.

Carlos Augusto Monteiro, Geoffrey Cannon, Renata Bertazzi Levy, Jean-Claude Moubarac, Maria Laura C Louzada, Fernanda Rauber, Neha Khandpur, Gustavo Cediel, Daniela Neri, Euridice Martinez-Steele, Larissa Galastri Baraldi, and Patricia Constante Jaime. Ultra-processed foods: What they are and how to identify them. *Public Health Nutrition*, 22(5):936–941, 2019. doi: 10.1017/S1368980018003762.

Han-Na Nam, Su-Min Jeong, Su-Bin Kim, and Soo-Jin Choi. Comprehensive evaluation of the genotoxic potential of food additive titanium dioxide in human intestinal cell systems. *Foods*, 14, 2025.

Evelyn C Pielou. The measurement of diversity in different types of biological collections. *Journal of Theoretical Biology*, 13:131–144, 1966.

Fritz-Albert Popp. Biologie des Lichts: Grundlagen der ultraschwachen Zellstrahlung. 1984.

Fritz-Albert Popp and Lev V Beloussov. Integrative biophysics: Biophotonics. 2003.

Marten Scheffer, Jordi Bascompte, William A Brock, Victor Brovkin, Stephen R Carpenter, Vasilis Dakos, Hermann Held, Egbert H Van Nes, Max Rietkerk, and George Sugihara. Early-warning signals for critical transitions. *Nature*, 461(7260):53–59, 2009. doi: 10.1038/nature08227.

F John Service, George D Molnar, Jack W Rosevear, Eugene Ackerman, Lael C Gatewood, and William F Taylor. Mean amplitude of glycemic excursions, a measure of diabetic instability. *Diabetes*, 19(9):644–655, 1970.

Ashley Shade, Hannes Peter, Steven D Allison, Didier L Baho, Monika Berga, Helmut Bürgmann, David H Huber, Silke Langenheder, Jay T Lennon, Jennifer BH Martiny, et al. Fundamentals of microbial community resistance and resilience. *Frontiers in Microbiology*, 3:417, 2012. doi: 10.3389/fmicb.2012.00417.

Claude E Shannon. A mathematical theory of communication. *The Bell System Technical Journal*, 27(3):379–423, 1948.

Justin L Sonnenburg and Fredrik Bäckhed. Diet–microbiota interactions as moderators of human metabolism. *Nature*, 535(7610):56–64, 2016. doi: 10.1038/nature18846.

Peter Stolz, Jenifer Wohlers, and Gudrun Mende. Measuring delayed luminescence by FES to evaluate special quality aspects of food samples — an overview. *Open Agriculture*, 4:410–417, 2019. doi: 10.1515/opag-2019-0039.

Joel Thorarinson, Allison Hensgen, and Iulia Koplik. The coherence engine: A unified framework for measuring system organization across physical domains. *arXiv preprint*, 2026a.

Joel Thorarinson, Allison Hensgen, and Iulia Koplik. Recovery is not return to baseline: Coherence operators for measuring biological recovery signatures. *arXiv preprint*, 2026b.

David Zeevi, Tal Korem, Niv Zmora, David Israeli, Daphna Rothschild, Adina Weinberger, Orly Ben-Yacov, Dar Lador, Tali Avnit-Sagi, Maya Lotan-Pompan, et al. Personalized nutrition by prediction of glycemic responses. *Cell*, 163(5):1079–1094, 2015. doi: 10.1016/j.cell.2015.11.001.

Shira Zelber-Sagi, Dana Ivancovsky-Wajcman, Naomi Fliss-Isakov, Michal Hahn, Muriel Webb, Oren Shibolet, Revital Kariv, and Amir Tirosh. Ultra-processed food is associated with nonalcoholic fatty liver disease and its related factors in adults. *International Journal of Environmental Research and Public Health*, 19:237–249, 2022.